

Supporting Information for “Constraining 20th-century sea-level rise in the South Atlantic Ocean”

Thomas Frederikse¹, Surendra Adhikari¹, Tim J. Daley², Sönke Dangendorf³, Roland Gehrels⁴, Felix Landerer¹, Marta Marcos^{5,6}, Thomas L. Newton², Graham Rush⁴, Aimée B.A. Slangen⁷, Guy Wöppelmann⁸

¹Jet Propulsion Laboratory, California Institute of Technology, Pasadena, California, USA

²School of Geography, Earth and Environmental Sciences, Plymouth University, Plymouth, UK

³Old Dominion University, Norfolk, Virginia, USA & University of Siegen, Siegen, Germany

⁴Department of Environment and Geography, University of York, Heslington, York, UK

⁵IMEDEA (UIB-CSIC), Esporles, Spain

⁶Department of Physics, University of the Balearic Islands, Palma, Spain

⁷NIOZ Royal Netherlands Institute for Sea Research, department of Estuarine and Delta Systems, and Utrecht University,

Yerseke, The Netherlands

⁸LIENSs, Université de La Rochelle - CNRS, La Rochelle, France

©2020. All rights reserved.

Contents of this file

1. Text S1
2. Figures S1-S5
3. Tables S2, S4

Additional Supporting Information

1. Table S1. Swan Inlet diatoms.
2. Table S3. ¹⁴C measurements.

Text S1: reconstructing sea-level changes at Swan Inlet, Falklands

This supplementary document includes methods and data that underpin the proxy-based relative sea-level reconstruction for the Falkland Islands. The reconstruction was established by *Newton* [2017] from microfossils preserved in salt-sediments at Swan Inlet (51°49'34"S, 58°35'47"W) in East Falkland. The sea-level reconstruction involved three steps: (1) collecting modern micro-organisms from salt-marsh surface sediments to establish sea-level transfer functions; (2) establishing a chronology for a sediment core; (3) applying the sea-level transfer function to microfossils preserved in the core to reconstruct relative sea-level changes. Step 1 is described in full in a separate paper [*Newton et al.*, 2020].

Sea-level transfer functions

We established three surface transects to investigate the vertical distributions of micro-organisms (diatoms) which are known to be reliable sea-level indicators [*Barlow et al.*, 2013; *Shennan et al.*, 2015]. For height control a survey benchmark was established at the edge of the salt marsh from which relative elevations for all sample points were measured. We refer to this benchmark as Swan Inlet Datum (SID). Using a differ-

Corresponding author: Thomas Frederikse, thomas.frederikse@jpl.nasa.gov

ential Global Positioning System (dGPS) we determined that SID is 14.35 m above the reference WGS84 ellipsoid. A total of 39 surficial (0-1 cm) sediment samples were collected at ~4 cm vertical increments across an elevational range of 1.27 m. From these samples, diatoms were extracted, counted and identified. The distribution of modern diatoms is shown in Figure S1. The data sets of modern diatoms, with their elevations, were subjected to regression analyses in the software package C2 [Juggins, 2003] to establish sea-level transfer function models following Newton *et al.* [2020]. Figure S2 depicts the performance of the selected transfer function by comparing elevations of our surface samples predicted by the transfer functions with their actual (surveyed) elevations. The regressions indicate that the diatom sea-level transfer function is capable of reconstructing past sea levels with an average precision of ± 0.06 m (2 sigma).

Chronology

Following an extensive reconnaissance of the salt-marsh stratigraphy of Swan Inlet, a core from Swan Inlet (core SI-2, 51°49'33.759"S, 58°35'46.654"W) was selected for the sea-level reconstruction. The chronology for core SI-2 combines age determinations from ¹³⁷Cs radionuclide activity in the upper 15 cm of the core (Figure S3) and 12 AMS ¹⁴C age determinations (Table S3) on individual horizontally embedded plant fragments down to a core depth of 0.9 m. The ¹³⁷Cs profile in core SI-2 reveals a peak between 6-8 cm that is related to the maximum deposition (1963 CE) of ¹³⁷Cs produced by atmospheric nuclear weapons testing. Below the maximum, ¹³⁷Cs is present at reduced levels, down to a depth of 15 cm. Background ¹³⁷Cs levels are first exceeded at 10 cm, indicating the onset of nuclear bomb testing, and we assigned an age of 1954 CE to this level. Due to possible mobility of Cs, we also subjected several plant fragments to radiocarbon bomb-spike analysis. We analysed the core for ²¹⁰Pb, but activity was generally low or below the minimum detection limit to provide reliable age determinations. An age-depth chronology with 95% confidence limits (Figure S4) was derived from a Bayesian modelling approach using Bacon in R [Blaauw and Christen, 2011]. The sea-level reconstruction presented here is based on the upper 15 cm of the core (dated to 1908-2013 CE). Bacon could not fit all age measurements into the age-depth model, because three samples returned 'modern ages' (Figure S4); two of these (61889 and 61891) are in the top 15 cm of the core. The dated material in these samples may have included root or rhizome material of modern plants. Our age model for the top 15 cm of the core is controlled by the two ¹³⁷Cs markers and the radiocarbon measurements at 6.5 cm (61829), 7.5 cm (61887), 10 cm (61888) and 21 cm (61897). Age uncertainties are lowest between 1954 and 1963 and increase lower in the core (Figure S4, Table S2).

Sea-level reconstruction

Past sea levels were calculated by the transfer function for every centimeter in core SI-2 based on the fossil diatom assemblages (Figure S5, Table S1). All samples have good or close modern analogues, except for one sample (2 cm) which is marginally across the close/poor boundary as defined by Watcham *et al.* [2013]. Kemp and Telford [2015] recommend for diatom datasets a lower cut-off for acceptable analogues, which implies that we should treat the 5 'close' analogue samples (Figure S5) with caution. We have tested the effect of removing these proxy data by removing these samples and using the sea-level observations from Port Louis [Woodworth *et al.*, 2010] instead. For this experiment, we tied the 2006 index point to the Stanley tide gauge data and subsequently tied the Stanley and Port Louis observations using the levelling data as described in Woodworth *et al.* [2010]. This experiment gives a 20th-century sea-level trend (without any corrections) at the Falk-

lands of 1.84 [0.92 - 2.89] mm yr⁻¹ versus 1.63 [1.10 - 2.77] mm yr⁻¹ for the estimate based on the full proxy record. The numbers in brackets denote the 5-95 % confidence interval. Given these relatively small changes and the comparison to tide-gauge observations (Figure 2h), which does not suggest reliability issues with these samples, we have retained these index points in our sea-level reconstruction.

The age for each level, including its uncertainty, was determined by the age-depth modelling (Figure S4, Table S2). The vertical uncertainty of each data point combines several potential sources of error related to sampling processes and regression model uncertainties, expressed as:

$$E = \sqrt{E_{\text{thick}}^2 + E_{\text{surv}}^2 + E_{\text{tfun}}^2} \quad (1)$$

where E is the total vertical error and E_{thick} , E_{surv} , and E_{tfun} are component errors. Component errors are defined as follows. Thickness error (E_{thick}) relates to potential sub-sampling errors associated with measuring the thickness of samples. Here this is defined as half of the measured thickness, following [Shennan, 1986], and thus amounts to 0.005 m for 1 cm slices. Levelling errors are negligible, because all proxy sea-level data are from the same core which required only a single surveying measurement. The uncertainties associated with transfer function estimates of sample elevation (E_{tfun}) use the sample-specific root mean squared errors of prediction (RMSEP) calculated by the C2 software package [Juggins, 2003] using bootstrapping [Birks, 1995]. Component errors are assumed to be the mean values with normally distributed uncertainty and are multiplied by 1.96 to obtain the 95% confidence intervals. Vertical errors associated with post-depositional lowering as a result of sediment compaction are considered to be negligible for the upper section of the core [Brain *et al.*, 2011].

References

- Barlow, N. L., I. Shennan, A. J. Long, W. R. Gehrels, M. H. Saher, S. A. Woodroffe, and C. Hillier (2013), Salt marshes as late Holocene tide gauges, *Global and Planetary Change*, 106, 90–110, doi:10.1016/j.gloplacha.2013.03.003.
- Birks, H. (1995), Quantitative palaeoenvironmental reconstructions, in *Statistical Modelling of Quaternary Science Data. Technical Guide 5.*, edited by D. Maddy and J. Brew, pp. 161–254, Quaternary Research Association.
- Blaauw, M., and J. A. Christen (2011), Flexible paleoclimate age-depth models using an autoregressive gamma process, *Bayesian Analysis*, 6(3), 457–474, doi:10.1214/11-BA618.
- Brain, M. J., A. J. Long, D. N. Petley, B. P. Horton, and R. J. Allison (2011), Compression behaviour of minerogenic low energy intertidal sediments, *Sedimentary Geology*, 233(1-4), 28–41, doi:10.1016/j.sedgeo.2010.10.005.
- Juggins, S. (2003), C2 User Guide. Software for Ecological and Palaeoecological Data Analysis and Visualisation, *Tech. rep.*, University of Newcastle, Newcastle-upon-Tyne, UK.
- Kemp, A. C., and R. J. Telford (2015), Transfer functions, in *Handbook of Sea-Level Research*, edited by I. Shennan, A. J. Long, and B. P. Horton, pp. 470–499, John Wiley & Sons, Ltd, Chichester, UK, doi:10.1002/9781118452547.ch31.
- Newton, T. L. (2017), Holocene sea-level changes in the Falkland Islands: New insights into accelerated sea-level rise in the 20th Century, Ph.D. thesis, The University of Plymouth.
- Newton, T. L., W. R. Gehrels, R. M. Fyfe, and T. J. Daley (2020), Reconstructing Sea-level change in the Falkland Islands (Islas Malvinas) using salt-marsh

- foraminifera, diatoms and testate amoebae, *Marine Micropaleontology*, p. 101923, doi: 10.1016/j.marmicro.2020.101923.
- Shennan, I. (1986), Flandrian sea-level changes in the Fenland. II: Tendencies of sea-level movement, altitudinal changes, and local and regional factors, *Journal of Quaternary Science*, 1(2), 155–179, doi:10.1002/jqs.3390010205.
- Shennan, I., A. J. Long, and B. P. Horton (Eds.) (2015), *Handbook of Sea-Level Research: Shennan/Handbook of Sea-Level Research*, John Wiley & Sons, Ltd, Chichester, UK, doi:10.1002/9781118452547.
- Watcham, E. P., I. Shennan, and N. L. M. Barlow (2013), Scale considerations in using diatoms as indicators of sea-level change: Lessons from Alaska, *Journal of Quaternary Science*, 28(2), 165–179, doi:10.1002/jqs.2592.
- Woodworth, P. L., D. T. Pugh, and R. M. Bingley (2010), Long-term and recent changes in sea level in the Falkland Islands, *Journal of Geophysical Research*, 115(C9), doi: 10.1029/2010JC006113.

Table S2. Proxy sea-level data for Swan Inlet (Falkland Islands). Age and vertical uncertainties denote the 95% confidence interval.

Depth (m)	Age (CE)	Age uncertainty (+)	Age uncertainty (-)	Sea level (m)	Sea level uncertainty (m)
0.01	2006	2012	1994	0.015	0.115
0.02	1999	2010	1985	0.038	0.128
0.03	1992	2005	1978	0.004	0.122
0.04	1985	2000	1972	-0.073	0.149
0.05	1978	1992	1967	0.062	0.109
0.06	1972	1985	1964	0.020	0.146
0.07	1964	1967	1961	-0.125	0.124
0.08	1961	1965	1956	-0.145	0.129
0.09	1957	1962	1953	-0.068	0.115
0.10	1954	1956	1951	-0.086	0.113
0.11	1945	1954	1928	-0.095	0.109
0.12	1936	1950	1913	-0.106	0.107
0.13	1926	1944	1901	-0.116	0.113
0.14	1917	1938	1889	-0.111	0.113
0.15	1908	1931	1876	-0.192	0.125

Table S4. Trends and uncertainties in mm yr^{-1} for each individual region and for the South Atlantic basin.

The numbers between brackets denote the 5-95% confidence intervals.

Region	No corrections	GIA correction	GIA + PD	Residual VLM	All corrections
Buenos Aires	1.53 [1.42 1.63]	2.15 [1.93 2.37]	2.21 [1.99 2.44]	1.79 [1.11 2.49]	2.48 [1.86 3.12]
Montevideo	1.55 [1.35 1.76]	2.11 [1.82 2.40]	2.12 [1.83 2.42]	1.25 [0.34 2.17]	1.82 [0.94 2.72]
Mar del Plata	1.23 [1.08 1.27]	1.66 [1.34 1.81]	1.76 [1.43 1.91]	0.74 [0.09 1.47]	1.26 [0.45 1.95]
Puerto Madryn	1.94 [1.68 2.29]	2.50 [2.18 2.91]	2.56 [2.21 3.00]	2.23 [0.81 3.84]	2.85 [1.43 4.43]
Dakar	1.13 [1.07 1.24]	1.19 [0.99 1.47]	1.35 [1.15 1.64]	1.17 [0.11 2.26]	1.38 [0.41 2.42]
South Africa	1.38 [1.24 1.52]	1.53 [1.38 1.67]	1.49 [1.35 1.64]	1.94 [1.69 2.15]	2.06 [1.78 2.27]
Kerguelen	1.10 [0.04 2.28]	0.94 [0.23 2.13]	0.93 [0.24 2.12]	2.19 [0.91 3.47]	2.02 [0.80 3.26]
Falklands	1.63 [1.10 2.77]	1.98 [1.43 3.14]	2.25 [1.63 3.33]	0.84 [0.06 2.31]	1.45 [0.52 2.81]
South Atlantic	1.48 [1.14 1.88]	1.78 [1.42 2.22]	1.93 [1.57 2.36]	1.13 [0.59 1.75]	1.61 [1.07 2.21]

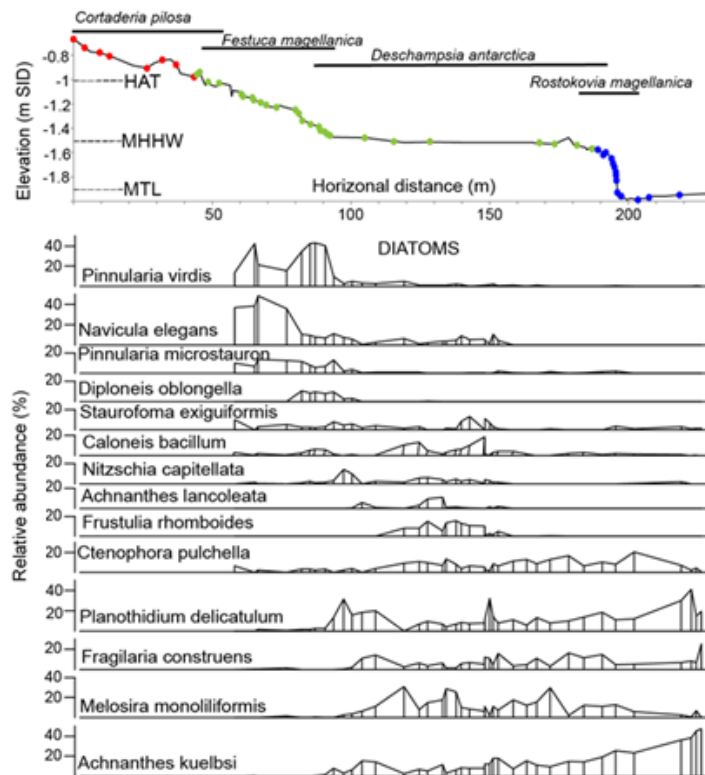


Figure S1. Distribution of modern diatoms in Swan Inlet. SID – Swan Inlet Datum. HAT - Highest Astronomical Tide. MHHW - Mean Higher High Water. MTL - Mean Tide Level. Samples were collected from three transects (as colour coded). Top panel shows the dominant plant species along the transects. From *Newton et al.* [2020].

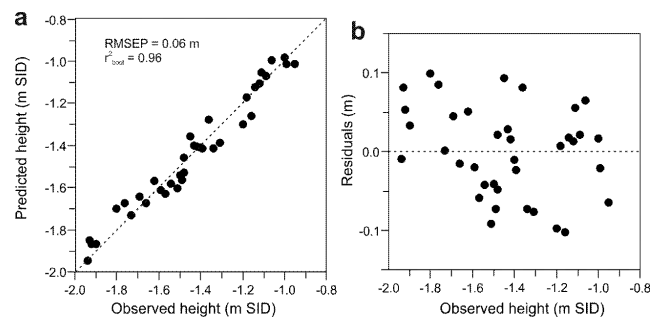


Figure S2. Scatterplot of observed versus predicted height (a) and observed height against prediction residuals (b) for the diatom transfer function using a Weighted Averaging Partial Least Squares (WA-PLS) model component 3. SID - Swan Inlet Datum. RMSEP - root mean squared error of prediction. From *Newton et al.* [2020].

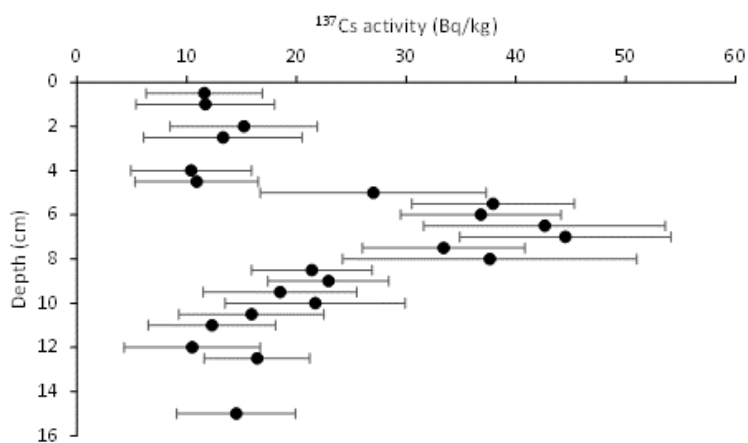


Figure S3. Profile of ^{137}Cs in core SI-2, showing the 1965 nuclear bomb testing maximum at 6-8 cm, and the 1954 onset of bomb testing at 9-11 cm.

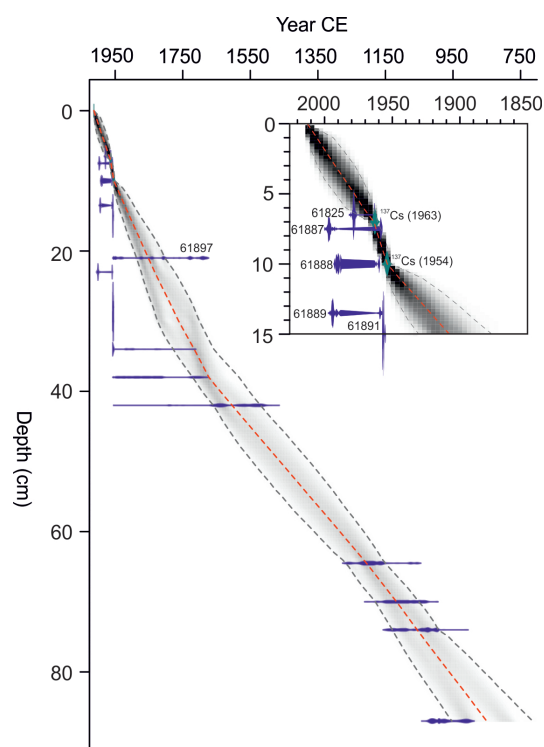


Figure S4. Age-depth chronology for core SI-2 (0-87cm) modelled by R-package Bacon [Blaauw and Christen, 2011], showing calibrated ^{14}C probability distributions (dark blue) and surface and ^{137}Cs ages (light blue). Darker greys indicate more likely calendar ages; grey dotted lines show 95% confidence intervals; red dotted line shows the single 'best' model based on the weighted mean age for each depth. For this paper, only the ages for the top 14 cm of the core were used. Laboratory codes correspond with Table S3.

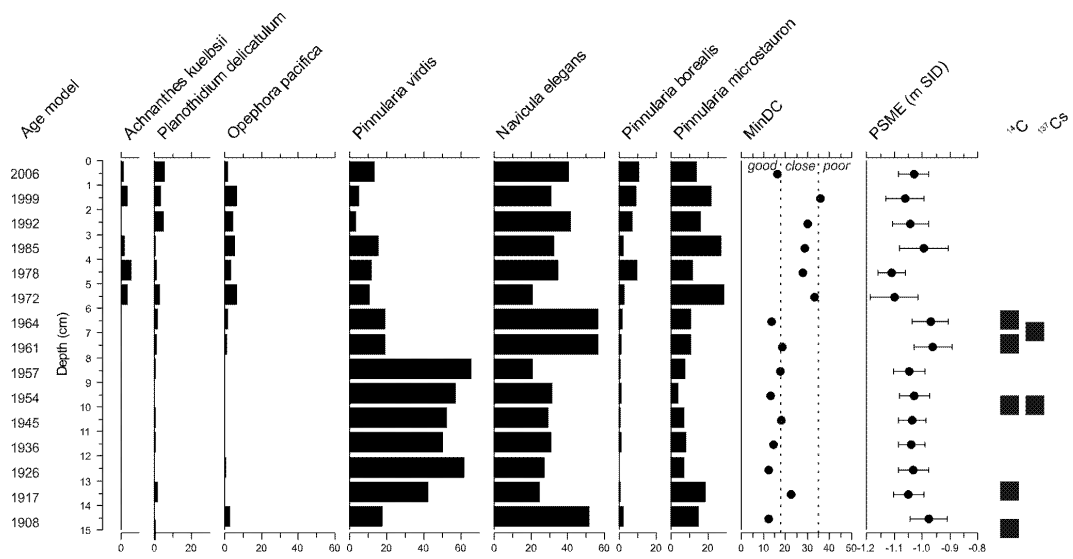


Figure S5. Fossil diatom assemblages, age markers and modelled ages in the top 15 cm of core SI-2 used for the sea-level reconstruction. Diatoms shown for species greater than 5% of the total valves counted. MinDC - minimum dissimilarity coefficient; definitions of 'good', 'close' and 'poor' follow *Watcham et al.* [2013]. PSME - palaeomarsh surface elevation. SID – Swan Inlet Datum.